Received: 10 February 2020 | Accepted: 15 April 2020

DOI: 10.1111/1365-2664.13649

RESEARCH ARTICLE

Journal of Applied Ecology BRITISH ECOLOGICAL SOCIETY

Unravelling the dispersal dynamics and ecological drivers of the African swine fever outbreak in Belgium

Simon Dellicour[1,2] | Daniel Desmecht[3] | Julien Paternostre[3] | Céline Malengreaux[4] | Alain Licoppe[4] | Marius Gilbert[1] | Annick Linden[3]

[1]Spatial Epidemiology Lab (SpELL), Université Libre de Bruxelles, Bruxelles, Belgium

[2]Department of Microbiology, Immunology and Transplantation, Rega Institute, KU Leuven, Leuven, Belgium

[3]FARAH Research Center, Faculty of Veterinary Medicine, University of Liège, Liège, Belgium

[4]Department of Environmental and Agricultural Studies, Public Service of Wallonia, Gembloux, Belgium

Correspondence
Simon Dellicour
Email: simon.dellicour@ulb.ac.be

Funding information
Public Service of Wallonia (Belgium); Fonds National de la Recherche Scientifique (FNRS, Belgium)

Handling Editor: Andrew Park

Abstract

1. African swine fever is a devastating disease of domestic pigs and wild boars caused by African swine fever virus (ASFV). ASFV originates from sub-Saharan African countries. In the last 10 years, the virus left its endemic range to spread to eastern Europe and Russia. On September 2018, Belgian authorities reported that ASFV had been detected in two wild boars in a southern area of the country. One year later, no domestic pig has been infected, with the last ASFV-positive wild boar being confirmed in mid-August 2019, suggesting that the outbreak is now controlled. However, the dispersal dynamics as well as the specific impact of ecological factors and intervention measures on the outbreak remain unknown.
2. In total, 827 positive cases have been reported in wild boar populations. In this study, we exploit the resulting spatio-temporal distribution of occurrence data to investigate the wavefront progression. We first present the application of recently developed methods to quantify the local wavefront velocity of an invading epidemic. Second, we develop and apply a novel analytical framework that uses occurrence data to investigate the impact of ecological factors on the dispersal dynamics of a wavefront progression.
3. Our analyses highlighted that the network of barriers, involving installed fences, had an impact on both the effective dispersal and the wavefront dispersal velocity. Furthermore, we also demonstrated that the wavefront progression was slower outside forest areas. Together, these results have concrete implications for potential future ASFV epidemics in similar regions.
4. *Synthesis and applications*. We describe a novel analytical approach that exploits occurrence data to investigate the impact of ecological factors on the wavefront velocity and actual wavefront progression. This methodology has the potential to be quickly applied to outbreak datasets solely made of occurrence data, with key benefits for the epidemiological investigations of external spatial factors impacting pathogen dispersal across non-endemic areas. Our analytical workflow could also be further applied to investigate the impact of ecological factors on any kind of biological dispersions (pathogen spreads, invasive species).

Simon Dellicour and Daniel Desmecht contributed equally to this work.

Marius Gilbert and Annick Linden contributed equally to this work.

KEYWORDS
African swine fever, biological invasion, dispersal dynamics, ecological factors, outbreak, virus, wavefront progression

1 | INTRODUCTION

African swine fever is a disease originally endemic to sub-Saharan Africa where it affects warthogs and domestic pigs, with soft tick species of the genus *Ornithodoros* acting as vectors (Chenais, Ståhl, Guberti, & Depner, 2018). The causative agent of the disease is the African swine fever virus (ASFV), a DNA virus belonging to the family Asfarviridae and genus *Asfivirus* (Galindo & Alonso, 2017) and for which there is currently no effective vaccine available (Sunwoo et al., 2019). In addition to its sub-Saharan African endemic range, the virus has also been circulating in Sardinia since 1978 (Mur et al., 2016). In 2007, it was introduced in Georgia and subsequently spread to the Russian Federation, Ukraine and Belarus and, in 2014, to the EU Baltic States and Poland (Callaway, 2012; Śmietanka et al., 2016). In 2017, the infection also affected both Czech Republic and Romania in 2017. Belgium, Hungary and Bulgaria were infected in 2018, as well as Slovakia and Serbia in 2019. The worst possible scenario occurred in 2018 when ASFV was detected in China, which contains half the world's swine population (Zhou et al., 2018). Widespread dissemination in China has been followed by spread to Mongolia, Vietnam, Cambodia, North Korea, South Korea, Myanmar, Laos and the Philippines (Dixon, Stahl, Jori, Vial, & Pfeiffer, 2020).

African swine fever virus dissemination could for instance be due to trade of live animals or pig products, transport of waste food or movement of contaminated materials (Roelandt, Van der Stede, D'hondt, & Koenen, 2015). ASF has one of the highest case-fatality rates among pig diseases and when it emerges in an uninfected country, it also has huge economic consequences due to the ban on exports (Andraud, Halasa, Boklund, & Rose, 2019; Gallardo et al., 2017; Guinat et al., 2018). While ASFV in Europe and eastern Russia initially followed a domestic cycle involving circulation among pig farms and some spillovers to wild boars, another cycle became progressively evident: a wild boar-habitat cycle, in which a wild boar population and its habitat act as a virus reservoir (Beltran-Alcrudo,

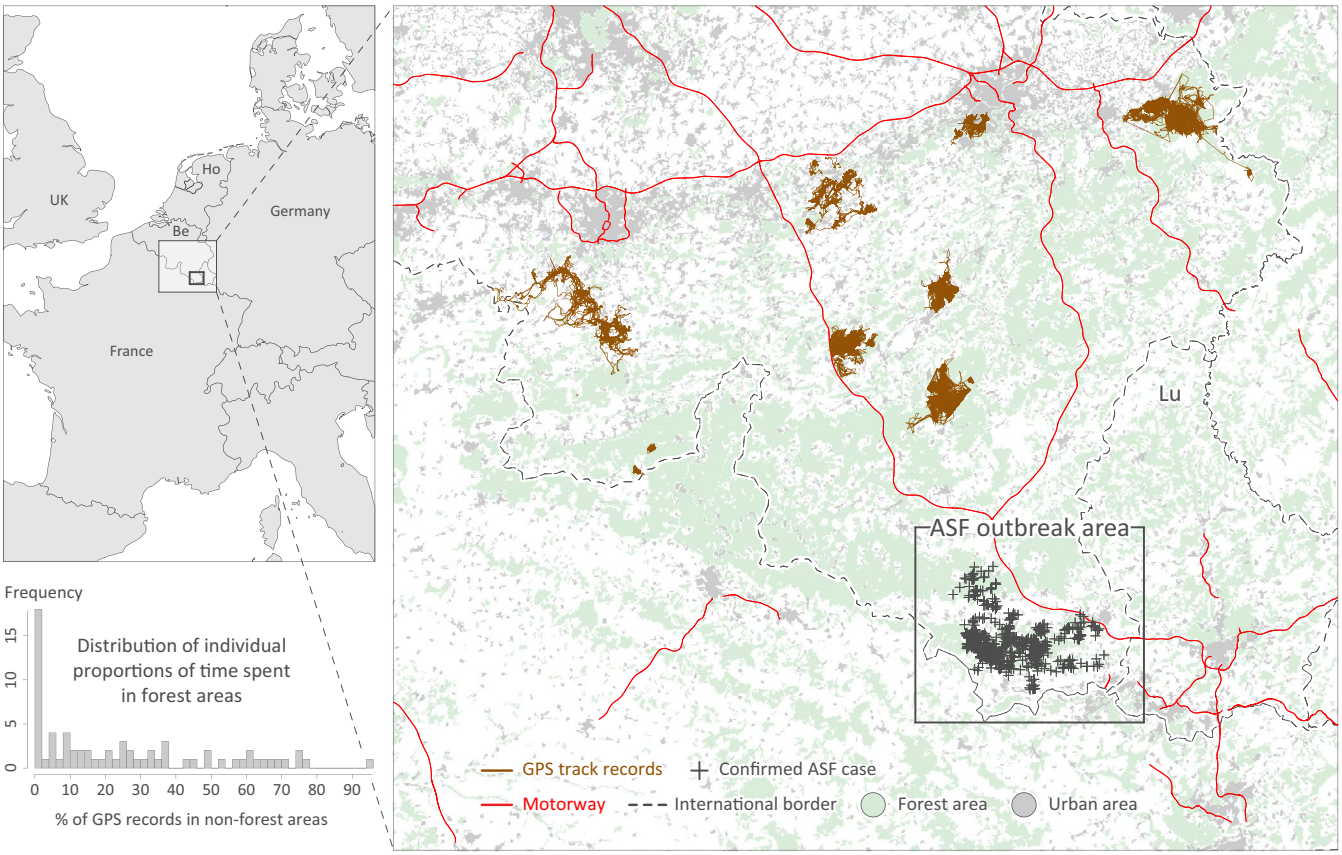

FIGURE 1 Study area, wild boar movement data, and localisation of African swine fever (ASF) cases. UK, United Kingdom; Be, Belgium; Ho, Holland; Lu, Luxembourg

Arias, Gallardo, Kramer, & Penrith, 2017; Chenais et al., 2018). In this cycle, infection routes can involve direct horizontal transmission, indirect transmission through contaminated environment (infected carcasses, excretions) or long-distance indirect transmission involving humans, for example through contaminated meat (Morelle, Jezek, Licoppe, & Podgorski, 2019; Roelandt et al., 2015).

On 13 September 2018, Belgian authorities reported that ASF had been confirmed in two wild boars in the province of Luxembourg in southern Belgium (Figure 1), located only 12 km from the border with France and 17 km from the country of Luxembourg (Linden et al., 2019). The genomes of the virus infecting these two first cases were partially sequenced in the context of a first phylogenetic analysis indicating that the causative strain belonged to genotype II and was thus related to strains previously isolated in Ukraine, Belarus and Estonia (Garigliany et al., 2019). This was further confirmed by the analysis of a complete genomic sequence (Gilliaux et al., 2019). Considering the geographic distance from these infected areas in eastern Europe, a human-mediated ASFV introduction was suspected (Beltran-Alcrudo, Falco, Raizman, & Dietze, 2019; Claude, 2018; Linden et al., 2019). In Belgium, while the emergence risk was estimated to be low, the disease consequences were deemed high (Roelandt et al., 2015), which was confirmed by the dramatic socio-economic consequences related to this outbreak on the Belgian territory (International Society for Infectious Diseases, 2019). Indeed, after its introduction, ASF has continued to spread in the wild boar population of southern Belgium, despite the implementation of strict control measures: complete standstill of any activity in the infected area, installation of fences aiming to restrict wild boar movements, active search for dead wild boars, removal of carcasses from the environment and intensive hunting of wild boars in the surrounding area (Andraud et al., 2019). However, after 11 months of ASF epidemic, the last fresh positive case was identified in August 2019.

While the combination of intervention measures seems to have been successful in controlling and containing the disease in the infected area, the dispersal dynamics as well as the specific impacts of ecological factors on the progression of ASF are still unknown. Understanding these aspects could be of crucial importance in the context of potential new outbreaks occurring in a similar environment, for example in western Europe. In the present study, we aimed to exploit the spatio-temporal dataset of confirmed infected cases to (a) analyse the dispersal history and dynamics of the ASFV in the wild boar population of southern Belgium and (b) unravel the impact of the main landscape features, that is the network of barriers and the forest coverage, on the wavefront progression and velocity. For this purpose, we implemented novel analytical procedures solely based on a collection of occurrence records. See Figure 2 for a detailed overview of the analytical workflow.

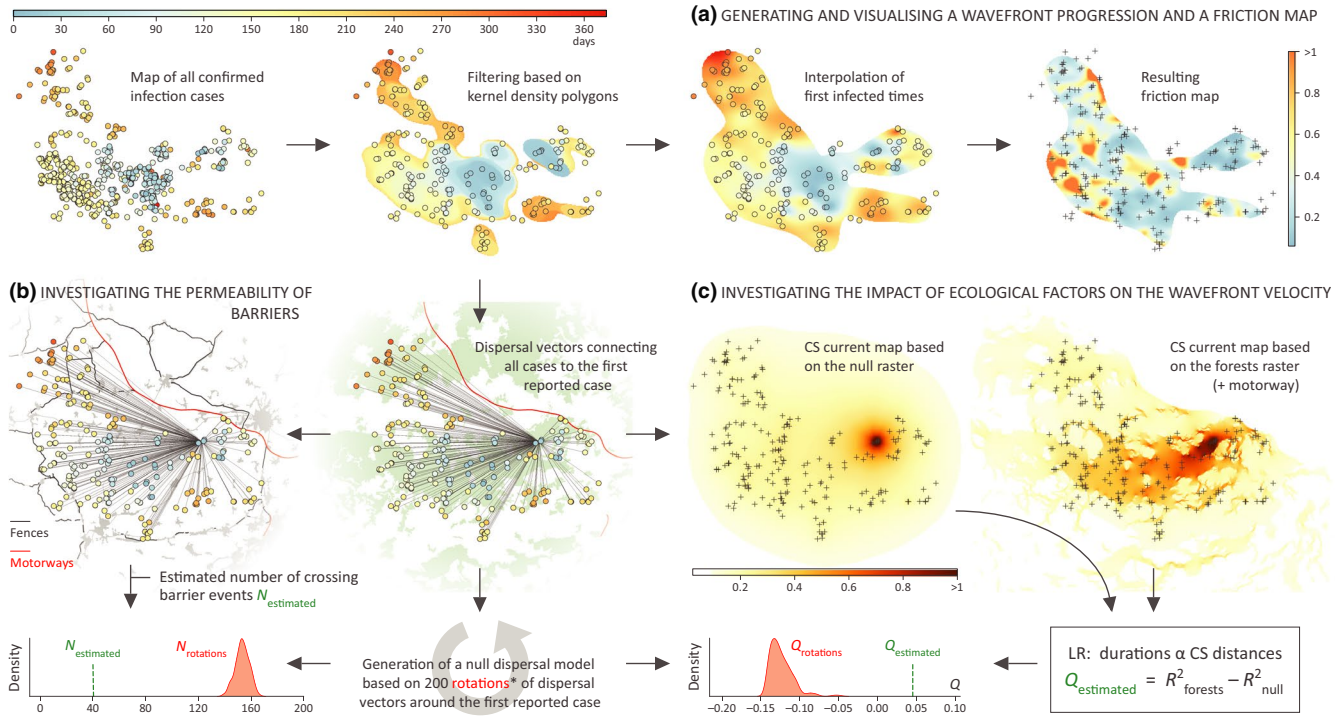

FIGURE 2 Analytical workflow implemented and applied to analyse the dispersal dynamics and drivers of the African swine fever virus (ASFV) outbreak in the wild boar population of southern Belgium. 'SL', 'CS', and 'LR' refer to 'straight-line', 'Circuitscape' and 'linear regression', respectively. Circuitscape cumulative current maps are here $\log_{10}$-transformed and obtained when connecting each infection case to the first detected case. These maps are thus illustrative of the Circuitscape path model used to compute the ecological distances involved in the linear regression analyses (similar tests were performed by considering the least-cost path model, see the text for further details). (*) Stochastic rotations of dispersal vectors were performed by respecting the proportion of filtered cases falling within (75.4%) or outside (24.6%) forest areas

2 | MATERIALS AND METHODS

2.1 | Preliminary analyses of wild boar movement data

We started by the preliminary analysis of wild boar movement data informed by GPS position records. Prior to the ASF outbreak (from 2003 to 2017), GPS collars had been placed on 76 individuals to track the movement of wild boars in different areas of southern Belgium (Figure 1). Each collar was set to register at least six fixes a day (Prévot & Licoppe, 2013). While no individual was tracked in the specific outbreak area, these data are informative on movement behaviours in the typical southern Belgian landscape alternating croplands and forest patches. We first used GPS records to check for crossing motorway events, simply by looking for intersections between straight-line segments connecting two successive GPS records and motorway segments. Secondly, we used GPS records to estimate the proportion of time each individual spent in forest areas. In practice, we used GPS positions to extract cell values on a forest coverage raster. We generated this forest coverage raster by starting from the categoric land cover raster of the CorineLandCover database (www.eea.europa.eu; resolution: ~100 m) and assigning a value of '0' or '1' for non-forest and forest raster cells respectively.

Thirdly, we used GPS records to investigate the impact of forest coverage on movement velocity. For each individual, we performed linear regressions between movement vector durations and forest coverage values extracted along straight-line segments formed by these movement vectors. The basic idea was to test if a significant proportion of the heterogeneity in movement velocity could be explained by the forest coverage. In practice, we estimated the statistic Q, which is here defined as the difference between two linear regression coefficients (R^2): (a) R^2_{forest} obtained from the linear regression $t \sim \Sigma v_{\text{forest}}$ between movement durations (t's) and the sum of forest raster cell values extracted along straight-line segments (Σv_{forest}) and (b) R^2_{null} obtained from the linear regression $t \sim \Sigma v_{\text{null}}$ between movement durations and corresponding raster cell value extractions performed on the 'null' raster (Σv_{null}), that is a uniform raster with the exact same resolution and extent but with a value of '1' assigned to all cells. The statistic Q ($=R^2_{\text{forests}} - R^2_{\text{null}}$) thus measures to what extent movement durations are best explained by ecological heterogeneity than solely by geographic distance (as measured by the sum of straight-line cell values extraction on the null raster). A statistic Q was estimated for each individual and tested using a null movement velocity model obtained by permuting durations among movement vectors. Estimated Q values were compared to their null distribution by a one-tail test to assess their level of significance. We tested the forest raster once as a potential conductance factor (increasing movement velocity) and once as a potential resistance factor (decreasing movement velocity). In the latter case, we thus tested the assumption of faster movements when individuals are more visible, that is evolving in-between forest areas. To test the forest raster as a potential conductance factor, raster cell values were inverted and R^2_{forest} was estimated from the linear regression $t \sim \Sigma(1/v_{\text{forest}})$. Inverting raster cell values to test an environmental raster as a conductance factor is a procedure used in least-cost path algorithm (Dijkstra, 1959) or in circuit theory (McRae, 2006), and allows to invert the relationship between dispersal durations and environmental values: higher environmental values will then be associated with lower dispersal durations. Furthermore, we also tested different values for the scaling parameter k defining the relationship between the original raster cell values and their conductance or resistance values (see below for further information on this scaling parameter). Because we obtained one p-value per individual and tested factor, we performed a Benjamini–Hochberg correction for multiple comparisons (Benjamini & Hochberg, 1995).

2.2 | Collecting and curating infection cases

The conditions of access to the infected area and the organization of the active search for dead wild boars are specified in the Walloon legislation. Search of carcasses is the responsibility of the regional authorities, which can call on collaborators like local hunters and landowners. Since the beginning of the outbreak, monitoring has been set up to map the surveyed areas and to quantify the research effort. Given the large size of the area, priorities have been established to guide surveillance to focus on certain zones. In the epidemic phase, passive surveillance mainly takes into account the proximity of outbreaks, the areas already covered in previous weeks and the boundaries of the infected area. When a carcass is discovered by the search teams, it is dated, geolocated and beaconed. The local forestry officer then calls the civil protection team especially dedicated for the extraction and packaging of the carcass under respect of biosecurity measures. This team also ensures the transport of the carcass to the collection centre where it will be handled by the team of veterinarians for sampling. Before sampling, carcasses are recorded (gender, weight, age class) and categorized into four decomposition categories (fresh, early decomposition, advanced decomposition and skeletonization) according to Brooks and Sutton's macroscopic criteria related to the level of decomposition (Brooks & Sutton, 2018). For consistency, this categorization is always performed by the same veterinary team and a checklist of macroscopic observations is systematically completed for each carcass. Recent works have shown how large a post-mortem interval determination can be (Brooks, 2016; Probst et al., 2020). Here, on the basis of field data (forest rangers) and expert opinion (veterinary pathologists) we have assigned at each stage a (sub-)categorical correction: +2 days for sanitary shots, −2 days for the 'fresh' stage with *rigor mortis*, −7 days for the 'early decomposition' stage, −14 days for the 'advanced decomposition' stage, −25 days for the 'skeletonization' stage without total disappearance of skin and ligaments, and −45 days for the 'skeletonization' stage with total disappearance of the above-mentioned organic elements and dry bones. Finally, targeted organs (spleen or long bones if organs are missing) are sent to the NRL for qPCR analysis and carcasses are transported to the rendering plant.

2.3 | Filtering infection cases, defining dispersal vectors

We estimated daily kernel density polygons to filter infection cases (Figure 2). For a given day *d*, we estimated the 95% kernel density polygon by considering the positions of all infection cases reported before *d*. We then used this series of daily polygons to discard infection cases that did not contribute in extending the outbreak area. Specifically, for a given day *d*, we only conserve infection cases occurring outside the kernel density polygon obtained for that day, that is, discarding infection cases detected in already infected areas. These filtered infection cases were subsequently used to visualize the wavefront progression and velocity, as well as to investigate the impact of ecological factors on the wavefront dispersal. For the latter analyses, we considered dispersal vectors by connecting all filtered cases to the first reported case, which was here used as an approximation of the outbreak origin. These dispersal vectors were all associated with a dispersal duration measured as the number of days separating the detection of a given case from the detection of the first case.

2.4 | Visualizing the wavefront progression and velocity

We started from the filtered infection cases to generate a visualization of the timely progression of the outbreak wavefront and a map reflecting local wavefront velocity (Figure 2a). For this purpose, we employed a previously described interpolation procedure (Kraemer et al., 2019; Tisseuil et al., 2016): (a) we used a thin plate spline regression to interpolate dates of filtered infection cases on a ~100 m resolution raster, (b) we measured the local slope of the interpolated surface with a 3 × 3 cells sliding window, (c) we further smoothed the resulting friction surface using an average 11 × 11 cells filter to prevent local null frictions values (Kraemer et al., 2019) and (d) we then estimated the local wavefront velocity by taking the inverse of the resulting friction value. To avoid extrapolation, we performed this procedure within a mask defined by the 95% kernel density polygon based on the positions of all reported infection cases.

2.5 | Generating a null dispersal model

We generated a null dispersal model by rotating dispersal vectors around their point of origin, that is, the first detected case (Figure 2). However, we performed these stochastic rotations under the constraint of respecting the proportion of filtered cases falling within or outside forest areas. With this null dispersal model, we thus generated infections cases sampled in realistic ecological conditions but under the assumption that ecological factors had no particular impact on dispersal durations. Indeed, while rotated, durations assigned to dispersal vectors are unchanged, no matter the new ecological conditions associated with the dispersal. Under this null dispersal model, we generated 200 datasets for subsequent analyses investigating the permeability of barriers as well as the impact of barriers and forests on the wavefront dispersal velocity.

2.6 | Investigating the permeability of barriers

To investigate the permeability of barriers, we compared the estimated number *N* of crossing barrier events with the distribution of numbers of such events obtained under the null dispersal model (Figure 2b). The tested barriers included the fences installed by the authorities during the outbreak, as well as already existing landscape features considered as a prior effective barrier to wild boar dispersal: main roads, urban areas and the motorway segment crossing the study area. We defined a crossing barrier event by an intersection between the straight-line formed by a dispersal vector and a barrier segment. We considered *N* as an *estimated* number of crossing barrier events because counting the number of crossing barrier events along straight-line dispersal vectors remained a simplification. However, we assumed that such an estimation was a reasonable proxy for the true number of times that the transmission chain did cross these barriers. Furthermore, the same metric was computed on the datasets generated under the null dispersal model. Therefore, if *N* overestimates the true number of crossing barrier events, it would also be the case in the null dispersal model, making *N* comparable to its null distribution to assess the permeability of barriers. In the one-tail test comparing the estimated *N* against its null distribution, the null hypothesis is that dispersal vectors did not cross barriers less often than expected by chance in the null dispersal model (Figure 2).

2.7 | Investigating the impact of ecological factors on the wavefront velocity

We further used the dispersal vectors to investigate the impact of different ecological factors on the wavefront velocity (Figure 2c). Here, we tested two different ecological factors formalized as rasters, that is geo-referenced grids containing ecological values: the forest coverage and the barriers defined above (Figure 2c). For that purpose, we adapted a methodology initially developed in landscape phylogeography to analyse the impact of ecological factors on the dispersal velocity of viral lineages (Dellicour et al., 2017; Dellicour, Rose, & Pybus, 2016). Specifically, we estimated the correlation statistic *Q*, which is here defined as the difference between two linear regression coefficients (R^2): (a) R^2_{eco} obtained from the linear regression $t \sim d_{\text{eco}}$ between time durations (*t*'s) and ecological distances (d_{eco}) computed on the ecological raster (i.e. geo-referenced grid of ecological values) and (b) R^2_{null} obtained from the linear regression $t \sim d_{\text{null}}$ between time durations (*t*'s) and ecological distances (d_{null}) computed on the corresponding null raster that is, as defined above, a uniform raster with a value of '1' assigned to all cells. Ecological distances were computed following two different path models: the least-cost (Dijkstra, 1959) and Circuitscape (McRae, 2006) path

models. The basic idea behind the statistic Q ($=R^2_{eco} - R^2_{null}$) is to measure to what extent the ecological raster better explains the heterogeneity in dispersal velocities than a homogeneous raster that only accounts for geographical distances in the path models. The barriers raster was here tested as a resistance factor and was obtained by projecting barrier features on the null raster by assigning a value of $1 + k$ to each raster cell crossed by a barrier. The so-called scaling parameter k was also used to transform the initial binary forest coverage raster into a conductance raster to be tested with the two different path models. In practice, forest raster cells were assigned a conductance value equal to $1 + k$, while non-forest raster cell values were assigned a conductance value of '1'. In both cases, we tested three different values for the scaling parameter k, that is, 10, 100 and 1,000, which allowed to control to what extent the ecological feature is more conductive (in the case of the forest raster) or more resistant (in the case of the barriers raster) than the absence of this ecological feature (Dellicour, Vrancken, Trovão, Fargette, & Lemey, 2018; Laenen et al., 2016). For both the forest and barrier rasters, we selected the k value maximizing the Q statistic. Finally, the level of significance of the estimated Q value was again tested using a one-tail test based on its comparison with the null distribution of Q values obtained under the null dispersal model (Figure 2). In this test, the null hypothesis is that the correlation between dispersal durations and ecological distances is not higher than the correlation values estimated under the null dispersal model where the ecological factors had no particular impact on the dispersal velocity. Because the motorway segment is an apparent effective barrier to ASF and wild boar dispersal, which is also confirmed by the analysis of individual capture–mark–recapture (Dellicour et al., 2019) and GPS data, the forest raster was preliminary modified to assign a very low conductance value ($1/[1{,}000 \times k]$) to raster cells crossed by the motorway segment.

3 | RESULTS

3.1 | Preliminary analyses of wild boar movement data

With the absence of detected crossing motorway events, even for individuals having their home range immediately next to a motorway, the GPS data further confirmed the significant impact of motorways on the dispersal frequency of these individuals, which was previously demonstrated with capture–mark–recapture data (Dellicour et al., 2019). The analysis of GPS movement data also revealed that on average, individuals spent ~74% of their time in forest areas, with ~59% of them spending at least 75% of their time in forest areas (Figure 1). As described in Section 2, we then analysed movement velocity by considering individual collections of movement vectors defined by successive position records. Specifically, we tested if movement velocity was significantly higher or lower in forest areas. Our analyses performed for each individual considered separately did not highlight such a trend. Taken together, these results thus formally confirm that, while these animals tend to mainly progress in forest areas, they do not disperse slower or faster in open lands.

3.2 | Collecting and curating infection cases

Between 11 September 2018 and 12 August 2019, 2,007 animals originated from the outbreak area have been tested for ASFV by qPCR. These animals were either culled (50.5%), found dead (44.2%), killed by road accidents (3.6%) or shot for sanitary reason (suspected to be infected; 1.6%). Among these tested animals, 827 (41.2%) were found positive for ASFV (96.3% found dead). The date of death was estimated for all individuals tested as positive for ASFV and used in subsequent analyses to date of all cases in number of days since the first detected case. As summarized in Figure 2, positive cases were all geo-referenced and used to analyse the dispersal dynamics and ecological factors having impacted the wavefront progression of ASFV in southern Belgium.

3.3 | Visualizing the wavefront progression and velocity

As reported in Figure 3, we visualized the progression of the wavefront by interpolating the first invasion times. These first invasion times were obtained by successive daily kernel density polygons to filter infection cases and only select those who actually extended the outbreak area (Figure 2). The filtering step discarded 582 (70.4%) of reported cases, resulting in a series of 245 conserved infection cases. As detailed in Section 2, interpolated first invasion times were then used to estimate a friction surface (time/distance; Figure 3). Finally, we estimated an overall wavefront velocity of 0.39 km/week by averaging the inverse of friction values. While interpolated first invasion times tend to indicate a relatively fast east to west invasion throughout the initially infected forest area, the visual association between forest coverage and wavefront friction appears less straightforward to interpret, calling for further formal investigations detailed below.

3.4 | Investigating the permeability of barriers

In addition to generating interpolation and friction surfaces, filtered cases were used to analyse the permeability of barriers to ASF dispersal. Under the term 'barriers', we included three different kinds of features: (a) fences installed by the authorities during the outbreak, (b) the motorway segment crossing the study area and (c) the roads or urban areas along which no fence was installed (Figure 3). Together, these barriers delimited closed areas that could potentially have contained ASF progression. Therefore, one initial question was the efficiency of this barrier network in actually blocking or not the spatial progression of the invasion. As described in Section 2, we considered the dispersal vectors connecting all filtered cases to the first detected

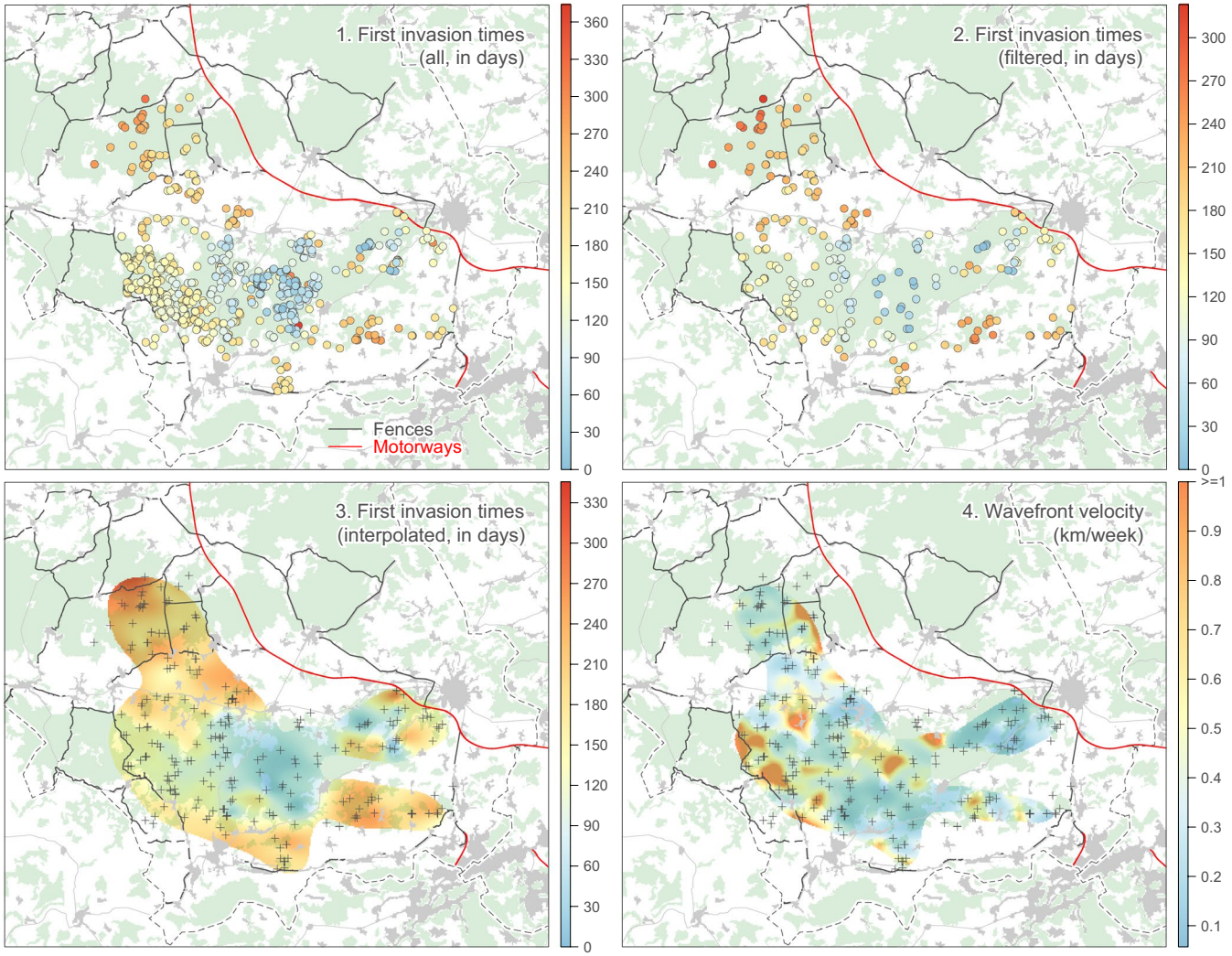

FIGURE 3 Analysis and visualisation of the wavefront velocity of the African swine fever virus (ASFV) outbreak in the wild boar population of southern Belgium. As detailed in the text, this figure displays and summarises the four analytical steps used to estimate the wavefront velocity across the study area: (1) collecting and mapping the first invasion times obtained from surveillance data, (2) using successive kernel density polygons to filter first invasion times by discarding reported cases occurring within already infected area, (3) interpolating first invasion times based on filtered cases (now represented by crosses), and (4) estimating a wavefront velocity map based on the interpolated invasion times map. Forest and urban areas are displayed in light green and grey, respectively, and international borders are represented by dashed lines

case, and estimated the number N of filtered cases that involved at least one crossing barrier event. To test if that estimated number of $N = 40$ crossing barrier events was higher than expected by chance, we performed a one-tailed test by comparing it to a distribution obtained following a null dispersal model (Figure 2). The test returned a $p < 0.001$, hence rejecting the null hypothesis in which barriers had no impact on dispersal frequency between fragmented areas.

3.5 | Investigating the impact of ecological factors on the wavefront velocity

We further used the dispersal vectors to investigate the impact of ecological factors on the wavefront velocity (Figure 2). As described in Section 2, we estimated the statistic Q measuring the proportion of the heterogeneity in dispersal velocities that can be associated with a given ecological factor, and assessed its level of significance using a one-tail test based on the null dispersal model. Our analyses revealed that the forest and barrier factors are both significant conductance and resistance factors to wavefront dispersal respectively. In other words, they are factors impacting the wavefront velocity as follows: the wavefront progressed faster within forest areas and was significantly slowed down by the presence of barriers, for which the significant permeability was already demonstrated above (Figure 4). In particular, considering the forest coverage raster rather the null raster allowed to increase by almost 20% of the amount of variation in wavefront velocity that can be explained by that particular ecological heterogeneity (Figure 4).

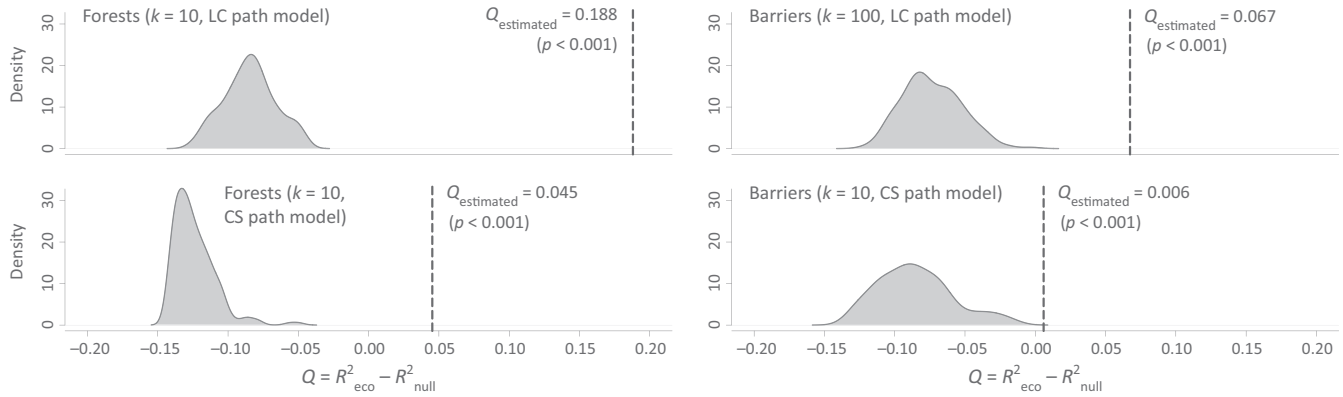

FIGURE 4 Analysis of the impact of ecological factors on the wavefront velocity of the African swine fever virus (ASFV) outbreak in the wild boar population of southern Belgium. Each graph reports the estimated value and null distribution of the correlation metric *Q*, which is defined as the difference between two linear regression coefficients (R^2): (1) R^2 obtained from the linear regression between time durations and ecological distances computed on the ecological raster (R^2_{eco}) and (2) R^2 obtained from the linear regression between time durations and ecological distances computed on the corresponding null raster (R^2_{null}). The null raster is a uniform raster presenting the exact same dimension and resolution as the ecological raster, but with a value of '1' assigned to all cells. Time durations are measured as the number of days separating each infection case with the first detected case, and ecological distances have been computed following two different path models: the least-cost ('LC') and Circuitscape ('CS') path models. *k* refers to the scaling parameter value used to transform the original ecological raster into a potential conductance (in the case of the forests raster) or resistance factor (in the case of the barriers raster) to dispersal velocity. The null distributions were obtained by reestimating the *Q* metric on infection cases generated according to a null dispersal model based on stochastic rotations of dispersal vectors (see the text for further details)

4 | DISCUSSION

The current ASF epidemic that is spreading through Asia is unprecedented in its magnitude (Food and Agriculture Organisation, 2019), with millions of pigs that died or were culled and profound implications in the broader livestock sector, with shift in production and consumption patterns towards poultry meat, for example. It will also likely influence the structure of the pig production sector with an accelerated shift towards intensive pig production systems that can implement biosecurity measures more easily, and reinforce the previously observed disappearance of small-scale producers (Thanapongtharm et al., 2016). In the countries affected by this large-scale epidemic, transmission predominantly results from human activities linked to the production and trade of pig meat through the value chain, and the relative importance of wild boars in spreading the disease is unknown. However, in several countries that have the capacity to enforce strict prevention and control measure of ASF in the pig production sector, the circulation of ASF in the wild boar population remains an important factor allowing the persistence and spread of the disease in domestic pigs (Jurado et al., 2018). In Asia, soon after the findings of the first pig farm infected by ASF in South Korea, wild boars infected by ASF were found in the demilitarized zone that separates the two Koreas, which suggested that they may have played a role in the cross-border transmission from North Korea (BBC News, 2019). So, although the relative role of wild boar and pig farming in the transmission of ASF may vary from country to country, what remains is that the persistence of the disease in the wild boar population may compromise the best efforts made in the pig production sector, and a good understanding of the factors influencing ASF dynamics in wild boar population is therefore essential.

For several reasons, controlling ASF in wild boar populations is particularly challenging (Claude, 2018; Linden et al., 2019). However, after 12 months of active intervention measures (controlled access to the infected area, dissemination of biosecurity principles, systematic removal of carcasses, depopulating wild boar, installing a network of fences), the Belgian outbreak in wild boars is no longer progressing. Therefore, the public authorities facing the disease elsewhere in the world could think of adapting their strategies according to the factors that slowed down the spatial extension of the infection.

In that context, our analyses formally demonstrate the efficiency of the installed network of fences. Complemented by pre-existing barriers (roads, urban areas), this network has impacted both the effective ASFV dispersal and the wavefront velocity. Our analyses also confirm that ASF progression was related to the forest habitat of wild boars. Indeed, the wavefront velocity was higher within forest areas and needed more time to cross non-forest areas. As indicated by the analysis of wild boar movement using GPS collars, this heterogeneity in wavefront velocity cannot be a priori explained by a difference in movement velocity of animals inside or outside forest areas. However, GPS movement data also inform us on the expected less frequent movement outside a forest environment. This latter result is in line with a scenario where open land actually slow down the ASF progression throughout a non-continuous wild boar population. Therefore, in the context of an ASF outbreak, considering the forest coverage pattern is of strategic importance to install fences and delimiting the area of containment.

We acknowledge that we cannot estimate the amount of missed infection cases. However, we hypothesize that these missed infections should have a minor impact on the statistical performances of

our analyses. Indeed, our null dispersal model generated by a randomization procedure mimics selected data, which here consist in ASFV records extending the infected area. This observed dataset is thus compared with randomized datasets associated with the same sampling effort, that is the same distribution of geographic distances between the first record case and cases extending the infected area. Therefore, the sampling pattern/effort should not have the potential to induce type I errors (false positive) but could, to some extent, reduce the statistical power of detection. However, we do not think that this was the case here as we did detect the impact of both barriers and forest coverage on the wavefront dispersal velocity.

Furthermore, we also acknowledge that our approach is sensitive to temporal uncertainty. By artificially leading to artefactual slower or faster local dispersal, uncertain or erroneous first invasion times estimated from the dates of death could indeed affect the accuracy of the results. The rate of post-mortem process is variable and highly affected by environmental conditions (e.g. temperature, moisture, insect activity, scavengers) and animal disposition factors (body size, body condition, body position, cause of death; Brooks, 2016). Most forensic studies are carried out on humans and pigs with specific parameters to estimate the date of death, but very limited data are actually available for wild boars (Probst, Globig, Knoll, Conraths, & Depner, 2017). Furthermore, a recent study demonstrated that decomposition rates of wild boar carcasses differed considerably from that of a domestic pig (Probst et al., 2020). In our study, carcasses were categorized into four decomposition categories (fresh, early decomposition, advanced decomposition and skeletonization stage) according to macroscopic criteria related to the level of decomposition (Brooks & Sutton, 2018). For the first stages of post-mortem process, we presume that the estimated dates of death are reliable because criteria on fresh carcasses and those in early decomposition are easier to interpret. However, for the last stage (skeletonization), the uncertainty around the estimates is increasing. Previous studies demonstrated that skeletonization may take a few days in summer but can be longer in winter (Probst et al., 2020). While it is practically difficult to quantify it, we thus acknowledge an uncertainty associated for the estimated date of death for bone samples discovered between November 2018 and July 2019 (corresponding to 16% of the filtered cases used in our study, i.e. 40 bone samples among 245 filtered ASFV records). Because it only concerns 16% of filtered ASFV records used in our analyses, we hypothesize that this uncertainty should here have a limited impact and not influence the general trends highlighted by our results.

Besides its specific application to the ASFV outbreak in Belgium, the present analytical workflow could be applied to investigate the impact of ecological factors on any kind of biological dispersal (pathogen spread, invasive species, etc). Being solely based on a spatio-temporal collection of confirmed occurrence data, our approach could be particularly useful in the absence of genetic data, which are now commonly used to unravel the impact of landscape feature in landscape genetic (Balkenhol, Waits, & Dezzani, 2009; Manel & Holderegger, 2013; Manel, Schwartz, Luikart, & Taberlet, 2003) or landscape phylogeographic studies (Brunker et al., 2018; Dellicour et al., 2018; Jacquot, Nomikou, Palmarini, Mertens, & Biek, 2017). Due to technical limitations, only a few ASFV genome sequences have been produced so far, and furthermore they show a very low level of genetic variability (Forth et al., 2019). In these circumstances, it is particularly challenging to exploit genetic information to study the impact of the ecological factors on the population structure and dispersal ability of the virus. This context has motivated the methodological developments applied and the present study, and we hope that it could be useful for further investigations of biological dispersals.

AUTHORS' CONTRIBUTIONS

S.D., D.D., M.G. and A.L.2 designed the study; D.D., J.P., C.M., A.L.1 and A.L.2 collected the data; D.D. and A.L.2 performed the experiments; S.D. and M.G. developed the analytical framework; S.D., D.D., A.L.1, M.G. and A.L.2 analysed the data; S.D. wrote the first draft of the manuscript; all the authors discussed the results and edited and approved the contents of the manuscript.

DATA AVAILABILITY STATEMENT

The GPS track records, ASFV occurrence data and all the R scripts for our analyses are available via the Zenodo Repository: https://doi.org/10.5281/zenodo.3764823 (Dellicour et al., 2020).

REFERENCES

Andraud, M., Halasa, T., Boklund, A., & Rose, N. (2019). Threat to the French swine industry of African swine fever: Surveillance, spread, and control perspectives. *Frontiers in Veterinary Science*, *6*. https://doi.org/10.3389/fvets.2019.00248

Balkenhol, N., Waits, L. P., & Dezzani, R. J. (2009). Statistical approaches in landscape genetics: An evaluation of methods for linking landscape and genetic data. *Ecography*, *32*(5), 818–830. https://doi.org/10.1111/j.1600-0587.2009.05807.x

BBC News. (2019). Boar with swine fever found in Korea border zone. *BBC News*. Retrieved from https://www.bbc.com/news/world-asia-49916065

Beltran-Alcrudo, D., Arias, M., Gallardo, C., Kramer, S. A., Penrith, M.-L., & Food and Agriculture Organization of the United Nations. (2017). *African swine fever: Detection and diagnosis–A manual for veterinarians*. Retrieved from http://www.fao.org/3/a-i7228e.pdf

Beltran-Alcrudo, D., Falco, J. R., Raizman, E., & Dietze, K. (2019). Transboundary spread of pig diseases: The role of international trade and travel. *BMC Veterinary Research*, *15*(1), 64. https://doi.org/10.1186/s12917-019-1800-5

Benjamini, Y., & Hochberg, Y. (1995). Controlling the false discovery rate: A practical and powerful approach to multiple testing. *Journal of the Royal Statistical Society: Series B (Methodological)*, *57*(1), 289–300. https://doi.org/10.1111/j.2517-6161.1995.tb02031.x

Brooks, J. W. (2016). Postmortem changes in animal carcasses and estimation of the postmortem interval. *Veterinary Pathology*, *53*(5), 929–940. https://doi.org/10.1177/0300985816629720

Brooks, J. W., & Sutton, L. (2018). Postmortem changes and estimating the postmortem interval. *Veterinary Forensic Pathology*, *1*, 43–63. https://doi.org/10.1007/978-3-319-67172-7_4

Brunker, K., Lemey, P., Marston, D. A., Fooks, A. R., Lugelo, A., Ngeleja, C., … Biek, R. (2018). Landscape attributes governing local transmission of an endemic zoonosis: Rabies virus in domestic dogs. *Molecular Ecology*, *27*(3), 773–788. https://doi.org/10.1111/mec.14470

Callaway, E. (2012). Pig fever sweeps across Russia. *Nature News*, *488*(7413), 565. https://doi.org/10.1038/488565a

Chenais, E., Ståhl, K., Guberti, V., & Depner, K. (2018). Identification of wild boar-habitat epidemiologic cycle in African swine fever epizootic. *Emerging Infectious Diseases*, *24*, 810–812. https://doi.org/10.3201/eid2404.172127

Claude, S. (2018). Unexpected discovery of African swine fever in Belgium. *Epidemiologie et Santé Animale*, *73*, 147–164.

Dellicour, S., Desmecht, D., Paternostre, J., Malengreaux, C., Licoppe, A., Gilbert, M., & Linden, A. (2020). Data from: Unravelling the dispersal dynamics and ecological drivers of the African swine fever outbreak in Belgium. *Zenodo Repository*, https://doi.org/10.5281/zenodo.3764823

Dellicour, S., Prunier, J. G., Piry, S., Eloy, M.-C., Bertouille, S., Licoppe, A., … Flamand, M.-C. (2019). Landscape genetic analyses of *Cervus elaphus* and *Sus scrofa*: Comparative study and analytical developments. *Heredity*, *123*(2), 228–241. https://doi.org/10.1038/s41437-019-0183-5

Dellicour, S., Rose, R., Faria, N. R., Vieira, L. F. P., Bourhy, H., Gilbert, M., … Pybus, O. G. (2017). Using viral gene sequences to compare and explain the heterogeneous spatial dynamics of virus epidemics. *Molecular Biology and Evolution*, *34*(10), 2563–2571. https://doi.org/10.1093/molbev/msx176

Dellicour, S., Rose, R., & Pybus, O. G. (2016). Explaining the geographic spread of emerging epidemics: A framework for comparing viral phylogenies and environmental landscape data. *BMC Bioinformatics*, *17*(1), 1–12. https://doi.org/10.1186/s12859-016-0924-x

Dellicour, S., Vrancken, B., Trovão, N. S., Fargette, D., & Lemey, P. (2018). On the importance of negative controls in viral landscape phylogeography. *Virus Evolution*, *4*(2), vey023. https://doi.org/10.1093/ve/vey023

Dijkstra, E. W. (1959). A note on two problems in connexion with graphs. *Numerische Mathematik*, *1*(1), 269–271. https://doi.org/10.1007/BF01386390

Dixon, L. K., Stahl, K., Jori, F., Vial, L., & Pfeiffer, D. U. (2020). African swine fever epidemiology and control. *Annual Review of Animal Biosciences*, *8*(1), 221–246. https://doi.org/10.1146/annurev-animal-021419-083741

Food and Agriculture Organisation. (2019). *One year on, close to 5 million pigs lost to Asia's swine fever outbreak*. Retrieved from http://www.fao.org/news/story/en/item/1204563/icode/

Forth, J., Forth, L., King, J., Groza, O., Hübner, A., Olesen, A., … Beer, M. (2019). A deep-sequencing workflow for the fast and efficient generation of high-quality African swine fever virus whole-genome sequences. *Viruses*, *11*(9), https://doi.org/10.3390/v11090846

Galindo, I., & Alonso, C. (2017). African swine fever virus: A review. *Viruses*, *9*(5), 103. https://doi.org/10.3390/v9050103

Gallardo, C., Soler, A., Nieto, R., Cano, C., Pelayo, V., Sánchez, M. A., … Arias, M. (2017). Experimental infection of domestic pigs with African swine fever virus Lithuania 2014 genotype II field isolate. *Transboundary and Emerging Diseases*, *64*(1), 300–304. https://doi.org/10.1111/tbed.12346

Garigliany, M., Desmecht, D., Tignon, M., Cassart, D., Lesenfant, C., Paternostre, J., … Linden, A. (2019). Phylogeographic analysis of African swine fever virus, western Europe, 2018. *Emerging Infectious Diseases*, *25*(1), 184–186. https://doi.org/10.3201/eid2501.181535

Gilliaux, G., Garigliany, M., Licoppe, A., Paternostre, J., Lesenfants, C., Linden, A., & Desmecht, D. (2019). Newly emerged African swine fever virus strain Belgium/Etalle/wb/2018: Complete genomic sequence and comparative analysis with reference p72 genotype II strains. *Transboundary and Emerging Diseases*, *66*(6), 2566–2591. https://doi.org/10.1111/tbed.13302

Guinat, C., Porphyre, T., Gogin, A., Dixon, L., Pfeiffer, D. U., & Gubbins, S. (2018). Inferring within-herd transmission parameters for African swine fever virus using mortality data from outbreaks in the Russian Federation. *Transboundary and Emerging Diseases*, *65*(2), 264–271. https://doi.org/10.1111/tbed.12748

International Society for Infectious Diseases. (2019). *African swine fever-Europe (53): Belgium (LX) wild boar, economic*. ProMED-mail post, archive number 20191126.6798858. Retrieved from https://promedmail.org/promed-post/?id=20191126.6798858

Jacquot, M., Nomikou, K., Palmarini, M., Mertens, P., & Biek, R. (2017). Bluetongue virus spread in Europe is a consequence of climatic, landscape and vertebrate host factors as revealed by phylogeographic inference. *Proceedings of the Royal Society B: Biological Sciences*, *284*(1864), 20170919. https://doi.org/10.1098/rspb.2017.0919

Jurado, C., Fernández-Carrión, E., Mur, L., Rolesu, S., Laddomada, A., & Sánchez-Vizcaíno, J. M. (2018). Why is African swine fever still present in Sardinia? *Transboundary and Emerging Diseases*, *65*(2), 557–566. https://doi.org/10.1111/tbed.12740

Kraemer, M. U. G., Reiner, R. C., Brady, O. J., Messina, J. P., Gilbert, M., Pigott, D. M., … Golding, N. (2019). Past and future spread of the arbovirus vectors *Aedes aegypti* and *Aedes albopictus*. *Nature Microbiology*, *4*(5), 854–863. https://doi.org/10.1038/s41564-019-0376-y

Laenen, L., Dellicour, S., Vergote, V., Nauwelaers, I., De Coster, S., Verbeeck, I., … Maes, P. (2016). Spatio-temporal analysis of Nova virus, a divergent hantavirus circulating in the European mole in Belgium. *Molecular Ecology*, *25*(23), 5994–6008. https://doi.org/10.1111/mec.13887

Linden, A., Licoppe, A., Volpe, R., Paternostre, J., Lesenfants, C., Cassart, D., … Cay, A. B. (2019). Summer 2018: African swine fever virus hits north-western Europe. *Transboundary and Emerging Diseases*, *66*(1), 54–55. https://doi.org/10.1111/tbed.13047

Manel, S., & Holderegger, R. (2013). Ten years of landscape genetics. *Trends in Ecology & Evolution*, *28*(10), 614–621. https://doi.org/10.1016/j.tree.2013.05.012

Manel, S., Schwartz, M. K., Luikart, G., & Taberlet, P. (2003). Landscape genetics: Combining landscape ecology and population genetics. *Trends in Ecology & Evolution*, *18*(4), 189–197. https://doi.org/10.1016/S0169-5347(03)00008-9

McRae, B. H. (2006). Isolation by resistance. *Evolution*, *60*(8), 1551–1561. https://doi.org/10.1554/05-321.1

Morelle, K., Jezek, M., Licoppe, A., & Podgorski, T. (2019). Deathbed choice by ASF-infected wild boar can help find carcasses. *Transboundary and Emerging Diseases*, *66*(5), 1821–1826. https://doi.org/10.1111/tbed.13267

Mur, L., Atzeni, M., Martínez-López, B., Feliziani, F., Rolesu, S., & Sanchez-Vizcaino, J. M. (2016). Thirty-five-year presence of African swine fever in Sardinia: History, evolution and risk factors for disease maintenance. *Transboundary and Emerging Diseases*, *63*(2), e165–e177. https://doi.org/10.1111/tbed.12264

Prévot, C., & Licoppe, A. (2013). Comparing red deer (*Cervus elaphus* L.) and wild boar (*Sus scrofa* L.) dispersal patterns in southern Belgium. *European Journal of Wildlife Research*, *59*(6), 795–803. https://doi.org/10.1007/s10344-013-0732-9

Probst, C., Gethmann, J., Amendt, J., Lutz, L., Teifke, J. P., & Conraths, F. J. (2020). Estimating the postmortem interval of wild boar carcasses. *Veterinary Sciences*, *7*(1), 6. https://doi.org/10.3390/vetsci7010006

Probst, C., Globig, A., Knoll, B., Conraths, F. J., & Depner, K. (2017). Behaviour of free ranging wild boar towards their dead fellows: Potential implications for the transmission of African swine fever. *Royal Society Open Science*, *4*(5), 170054. https://doi.org/10.1098/rsos.170054

Roelandt, S., Van der Stede, Y., D'hondt, B., & Koenen, F. (2015). The assessment of African swine fever virus risk to Belgium early 2014, using the quick and semiquantitative Pandora screening protocol.

Transboundary and Emerging Diseases, *64*(1), 237–249. https://doi.org/10.1111/tbed.12365

Śmietanka, K., Woźniakowski, G., Kozak, E., Niemczuk, K., Frączyk, M., Bocian, Ł., … Pejsak, Z. (2016). African swine fever epidemic, Poland, 2014–2015. *Emerging Infectious Diseases*, *22*(7), 1201–1207. https://doi.org/10.3201/eid2207.151708

Sunwoo, S.-Y., Pérez-Núñez, D., Morozov, I., Sánchez, E., Gaudreault, N., Trujillo, J., … Richt, J. (2019). DNA-protein vaccination strategy does not protect from challenge with African swine fever virus Armenia 2007 strain. *Vaccines*, *7*(1), 12. https://doi.org/10.3390/vaccines7010012

Thanapongtharm, W., Linard, C., Chinson, P., Kasemsuwan, S., Visser, M., Gaughan, A. E., … Gilbert, M. (2016). Spatial analysis and characteristics of pig farming in Thailand. *BMC Veterinary Research*, *12*(1), 218. https://doi.org/10.1186/s12917-016-0849-7

Tisseuil, C., Gryspeirt, A., Lancelot, R., Pioz, M., Liebhold, A., & Gilbert, M. (2016). Evaluating methods to quantify spatial variation in the velocity of biological invasions. *Ecography*, *39*(5), 409–418. https://doi.org/10.1111/ecog.01393

Zhou, X., Li, N., Luo, Y., Liu, Y. E., Miao, F., Chen, T., … Hu, R. (2018). Emergence of African swine fever in China, 2018. *Transboundary and Emerging Diseases*, *65*(6), 1482–1484. https://doi.org/10.1111/tbed.12989

How to cite this article: Dellicour S, Desmecht D, Paternostre J, et al. Unravelling the dispersal dynamics and ecological drivers of the African swine fever outbreak in Belgium. *J Appl Ecol*. 2020;00:1–11. https://doi.org/10.1111/1365-2664.13649